[EPSC2026-758]

Influence of the solar wind on the Venusian hydrogen upper atmosphere : SPICAV limb observations and radiative transfer modelling

Chizuru Nose[1](nose.c@pparc.gp.tohoku.ac.jp), K. Masunaga[2], F. Tsuchiya[1], S. Sakai[3], Y. Kasaba[1], S. Aoki[4,1], J-Y. Chaufray[5], F.Leblanc[5]
[1]Tohoku University, [2]Yamagata University, [3]Keio University, [4]University of Tokyo, [5]LATMOS/IPSL

Introduction

◆ The loss of water on Venus

The observation of H and O can previously impose constraints on the loss of water from the atmosphere.(Donahue et al., 1982) Variability in the oxygen airglow has been analyzed by Hisaki. (Masunaga et al., 2015,2017, Nara et al., 2020).

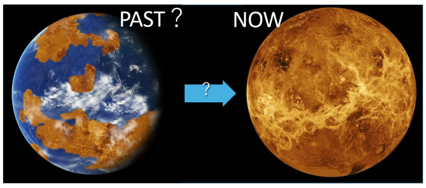

➤Oxygen atoms are products of not only water molecules but carbon dioxide, whereas hydrogen atoms are mostly produced by the dissociation of water molecules. Observation of hydrogen is essential for studying the loss of water.

◆ Venusian hydrogen exosphere

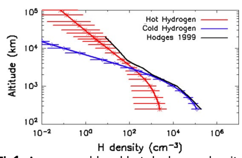

Fig1. Average, cold and hot hydrogen density in the exosphere near noon [Chaufray et al.,2012]

- The Venusian hydrogen exosphere consists of two populations with different scale heights (Wellance et al., 1967; Anderson et al., 1976; Chaufray et al., 2012, 2015).
- Because the thermal escape of cold hydrogen is negligible, the hot population plays the dominant role in atmospheric escape (Lammer et al., 2006).
- The hot component is thought to be produced by charge exchange between ionospheric ions and neutral atoms (Hodges et al., 1981, 1991, 1999).
- Hisaki observations have shown that hydrogen Ly-α brightness increases following the arrival of high-speed solar wind, likely due to an enhancement of the hot component; however, the influence of the solar wind on the hot component remains poorly understood (Nose et al, under review).

How are hot hydrogen atoms produced in the Venusian exosphere?

- Estimate the brightness of Venusian hydrogen airglow using ultraviolet spectroscopic observations from VEX/SPICAV.(Bertaux et al., 2007)
- Derive temperature and density by radiative transfer calculation.
- Investigate its variability in response to solar wind arrival.
- Using a Bayesian optimization to efficiently constrain the best-fit values and their uncertainties.

Method

◆ Observation

- In March 2014
  - High-speed solar wind arrived twice.
  - Both Hisaki and SPICAV were operating.
- Ly-α vertical profile

➤ from tangential point (TP) altitude vs. brightness

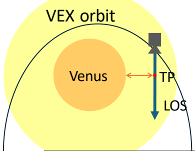

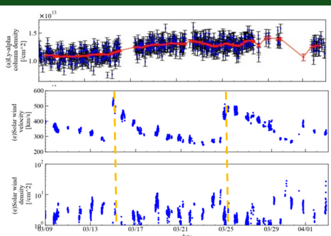

Fig. 2. Time series of Ly-alpha brightness observed by Hisaki, the solar wind velocity and density in March 2014 observed by ASPERA-4/VEX. The orange lines indicate the timing of the SPICAV limb observations (Nose et al, under review).

Table1 SPICAV observation geometry

	3/16	3/20 (Case A)	3/26 (Case B)
TP SZA[deg]	106	122	123
TP LT[h]	19.2	19.6	20.2
TP Alt[km]	581→1936	7728 →6790	-569 →9320

◆ Radiative transfer (RT) calculation

Monte Carlo radiative transfer model developed by Chaufray et al (Chaufray et al.,2008:2012:2015)

- **Exosphere**: Chamberlain Model
- **Below the Exobase** : Cold hydrogen is derived by solving the diffusion equation. Hot components are neglected.

➤Consistently simulates the volume emission rate from both cold and hot hydrogen.

Input parameters

- Cold H density(N_{cold}) /temperature (T_{cold}) @exobase(250km)
- Hot H density (N_{hot}) / temperature (T_{hot}) @ exobase
- Spacecraft position and LOS vectors

By fitting the observations with forward-modeled brightness, we can derive the density and temperature of exospheric hydrogen, separated into hot and cold components.

Result & Discussion

◆ SPICAV Limb observation

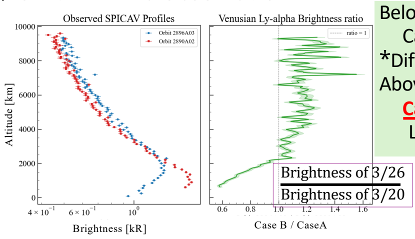

Fig 3. Observed Ly-α brightness altitude profile on Mar. 20 and 26.

Below 2,000 km
Case A (Mar.20) > Case B (Mar. 26)
*Difference of geometry
Above 2,000 km
Case A (Mar.20) < Case B (Mar.26)
Larger than error bar (1 min)

◆ Current RT best fit

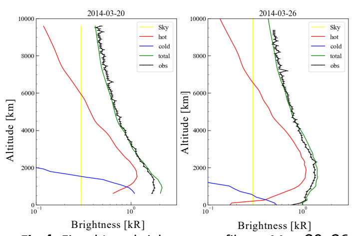

Fig 4. Fitted Ly-α brightness profile on Mar. 20, 26.

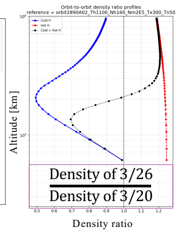

Fig 5. Profile of H density ratio (3/26 per 3/16)

After the arrival of CIR

- 10-50 % decreasing cold hydrogen density.
- **20 % increasing** hot hydrogen density.

◆ Bayesian optimization

- Goodness of Fit: $\chi^2 = \frac{1}{n-4}\sum\frac{(O_i - E_i)^2}{\sigma_i^2}$
- Computational Challenge
  - Grid search requires many iterations
  - ~4 hours needed for one parameter set

➤ Improve fitting efficiency while maintaining accuracy
➤ **Replace grid search with Bayesian optimization**

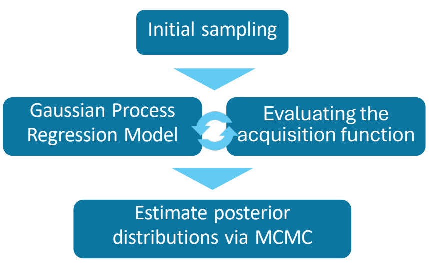

◆ Test case study for Bayesian optimization

Mock Ly-α brightness profiles were generated using radiative transfer calculations to test whether a Bayesian optimization loop converges to the true parameters and to assess the precision of the resulting posterior distributions.

- When exploring one parameter, with the other three fixed at their true values, the posterior median converged close to the true value in each case, with the truth falling within the 1σ credible interval.
- When all four parameters were varied simultaneously, however, recovery accuracy degraded, especially for the hot component parameters: N_{cold} converged to within 0.71σ, T_{cold} within 2.69σ, while N_{hot} deviated by 6.57σ and T_{hot} by 8.61σ. This indicates that the hot component parameters remain poorly constrained under multi-parameter optimization.

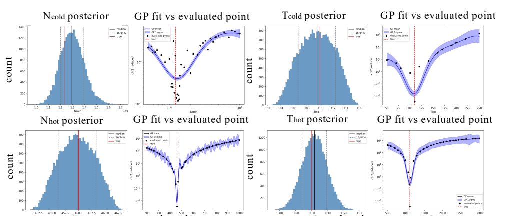

Fig 6. Posterior distributions (left) and Gaussian process (GP) surrogate fits to the reduced χ² (right) for the four fitted parameters .In each posterior histogram, the black line is the median, the grey dashed lines the 1σ, and the red line the true value. In each GP panel, black points show the reduced χ² at each evaluated parameter value, the blue curve the GP mean prediction, the shaded blue band the 1σ GP uncertainty.

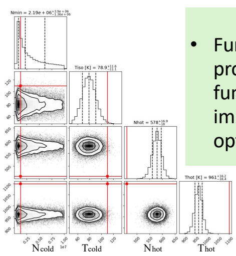

Fig 7. Corner plot of the joint and marginal posterior distributions from the four-parameter Bayesian optimization run. Diagonal panels show marginalized posteriors (median and 16th/84th percentiles); off-diagonal panels show 2D joint posteriors with 1σ/2σ/3σ contours. Red lines mark the true parameter values.

Future works

- Further tuning of the Gaussian process kernel and acquisition function, along with improvements to the Bayesian optimization loop.